Supporting Information

Degradation of chitin by a tri-modular enzyme that combines hydrolytic and oxidative cleavage of glycosidic bonds

Sophanit Mekasha[1], Tina Rise Tuveng[1], Fatemeh Askarian[1], Swati Choudhary[2], Claudia Schmidt-Dannert[2], Axel Niebisch[3], Jan Modregger[3], Gustav Vaaje-Kolstad[1], Vincent G. H. Eijsink[1,*]

[1]Faculty of Chemistry, Biotechnology and Food Science, Norwegian University of Life Sciences (NMBU), N-1432 Ås, Norway; [2]Department of Biochemistry, Molecular Biology and Biophysics, University of Minnesota, St. Paul, Minnesota 55108 USA; [3]Eucodis Bioscience GmbH, Campus Vienna Biocenter 2, 1030 Wien, Austria

Running title: A chitinolytic enzyme with hydrolytic and oxidative activity

[*]To whom correspondence should be addressed: Vincent G. H. Eijsink: Faculty of Chemistry, Biotechnology and Food Science Norwegian University of Life Sciences (NMBU), 1432 Ås, Norway; vincent.eijsink@nmbu.no; Tel. +47 67232463.

Supporting Information includes:

1. List of supporting Tables and Figures
2. Supporting Tables and Figures
3. Supporting discussion

1. LIST OF SUPPORTING TABLES AND FIGURES

Table S1. Primers used for the generation of truncated *Jd*1381 versions.

Table S2. Abundant proteins in the secretome of *J. denitrificans* grown on β-chitin.

Figure S1. SDS-PAGE analysis of proteins secreted by *J. denitrificans* grown on β-chitin.

Figure S2. Structural comparison of *Jd*Chi18 with the well-characterized chitinase *Sm*Chi18A from *Serratia marcescens*.

Figure S3. Kinetics of the degradation of chitopentaose by *Jd*1381 and *Jd*Chi18.

Figure S4. Time-dependent binding of *Jd*1381 variants to α-chitin (A) and β-chitin (B).

Figure S5. Comparison of *Jd*1381 with combinations of chitinases and an AA10-type LPMO from *Serratia marcescens* BJL200 in α-chitin hydrolysis.

2. SUPPORTING TABLES AND FIGURES

Table S1. Primers used for the generation of truncated *Jd*1381 versions. Restriction sites are underlined and stop codons are indicated in bold italics.

Cloning primers	**Sequence and Description**
pUCBB/JdLPMO10_F	5' CCGTAGCAATGGATCCATGAAGAAGAGAAAGTTGAGAGCGTCAGC 3'; forward primer used to clone *Jd*LPMO10 and *Jd*LPMO10-CBM5; *Bam*HI site underlined
pUCBB/JdLPMO10_R	5' TCGTAATGCCGCGGCCGC***TCA***TGAGACCACAACATCCATACAGTTG 3'; reverse primer used to clone *Jd*LPMO10; *Not*I site underlined
pUCBB/JdLPMO10-CBM5_R	5' GATGCTCGAGGCGGCCGC***TCA***AGGTGGAGTGCCACCTTCACCTGGG 3'; reverse primer used to clone; *Not*I site underlined
pET26b/JdCBM5-Chi18_F	5' CTGATCATATGCAGTGCCCACCGGCGTATAG 3'; forward primer used to clone *Jd*CBM5-Chi18; *Nde*I site underlined
pET26b/Chi18_F	5' CTGATCATATGGGTACGGGCGACGAGCGTATC 3'; forward primer used to clone *Jd*Chi18; *Nde*I site underlined
pET26b/Chi18_R	5' CTGATCTCGAGTTGGAGGCCCGTAGCAATGGC 3'; reverse primer used to clone *Jd*CBM5-Chi18 and *Jd*Chi18; *Xho*I site underlined

Table S2. The most abundant proteins in the secretome of *J. denitrificans* grown on β-chitin.
Proteins in the secretome were separated by SDS-PAGE, six bands were analyzed using LC-MS/MS, as indicated in Figure S1. The most abundant protein in each band, based on emPAI values from the Mascot Deamon search, is reported in the table.

Band number	Protein (Uniprot ID)	*J. denitrificans* gene ID
1	Chitinase (C7R4I0)	*Jden_1381*
2	Extracellular solute-binding protein family 1 (C7R2P1)	*Jden_2399*
3	Extracellular solute-binding protein family 1 (C7R2P1)	*Jden_2399*
4	Glyceraldehyde-3-phosphate dehydrogenase (C7R455)	*Jden1256*
5	Purine nucleoside phosphorylase (C7R2C6)	*Jden_0835*
6	Superoxide dismutase (C7R4P3)	*Jden_1450*

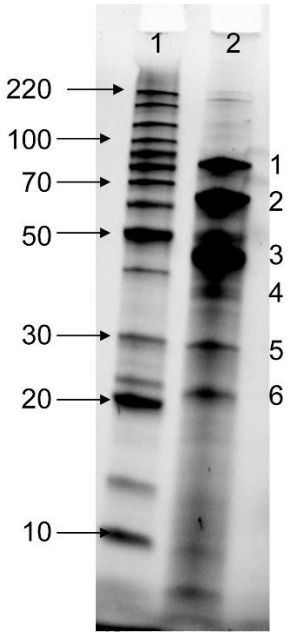

Figure S1. SDS-PAGE analysis of proteins secreted by *J. denitrificans* grown on β-chitin. Lane 1, protein marker with molecular masses indicated in kDa. Lane 2, 20x concentrated culture supernatant. The six protein bands selected for further investigation are indicated by numbers. *Jd*1381 was the most abundant protein in band 1 (see Table S2).

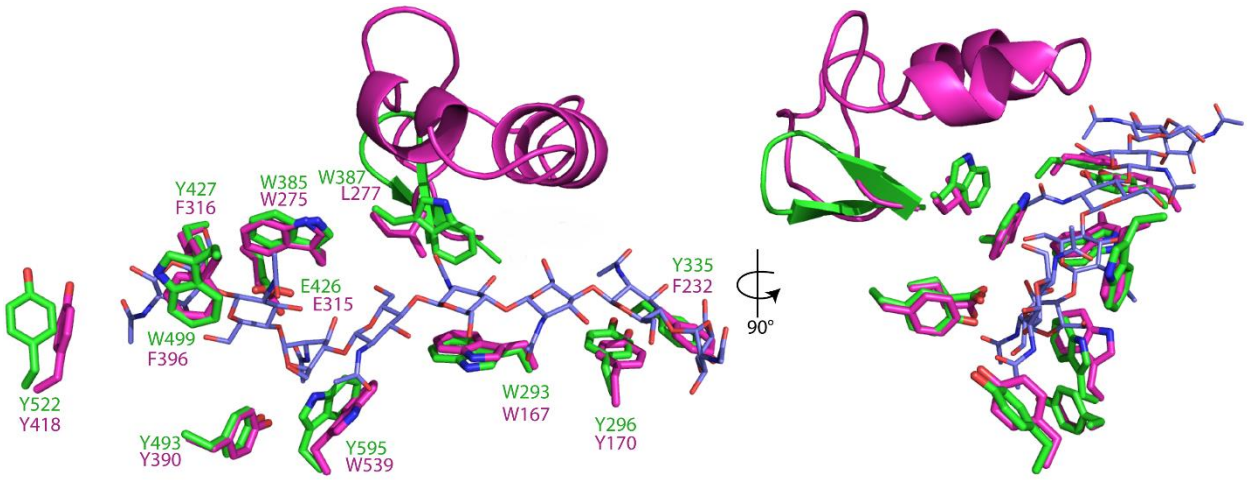

Figure S2. Structural comparison of *Jd*Chi18 with the well-characterized chitinase *Sm*Chi18A from *Serratia marcescens*. The picture shows a comparison of residues located in the catalytic center and substrate-binding cleft of the *Jd*Chi18 homology model (green carbons) and the *Sm*Chi18A X-ray crystallographic structure (pink carbons; PDB: 1EIB, (1)) containing chitooctaose (blue carbons). *Sm*Chi18A is a processive exo-chitinase acting from the reducing end of chitin chains (2-4); the chitooctaose occupies subsites -6 (to the right) to +2 (to the left). The side chains shown are the catalytic acid/base (E426 in *Jd*Chi18, E315 in *Sm*Chi18A) and aromatic residues for which studies of *Sm*Chi18A and other chitinases from *S. marcescens* have shown that they play a role in enzyme-substrate interactions and co-determine the degree of processivity (see (3,5,6) for more details). The figure shows that all residues, except L277 in *Sm*Chi18A, which is replaced by W387 in *Jd*Chi18, are similar between the two chitinases. The parts of the backbone that are shown in cartoon representation highlight a region where *Sm*Chi18A has an insertion relative to *Jd*Chi18 that gives the substrate-binding cleft of the former a more closed, almost "tunnel-like" character (this insertion is coloured cyan in Figure 2 of the main manuscript). The right panel shows the superposition after a 90º rotation around *y*-axis, to further illustrate the impact of this insertion on the substrate-binding cleft. The figures were made by pairwise superposition of the predicted *Jd*Chi18 structure with the crystal structure of the catalytic domain of *Sm*ChiA, using Pymol (7).

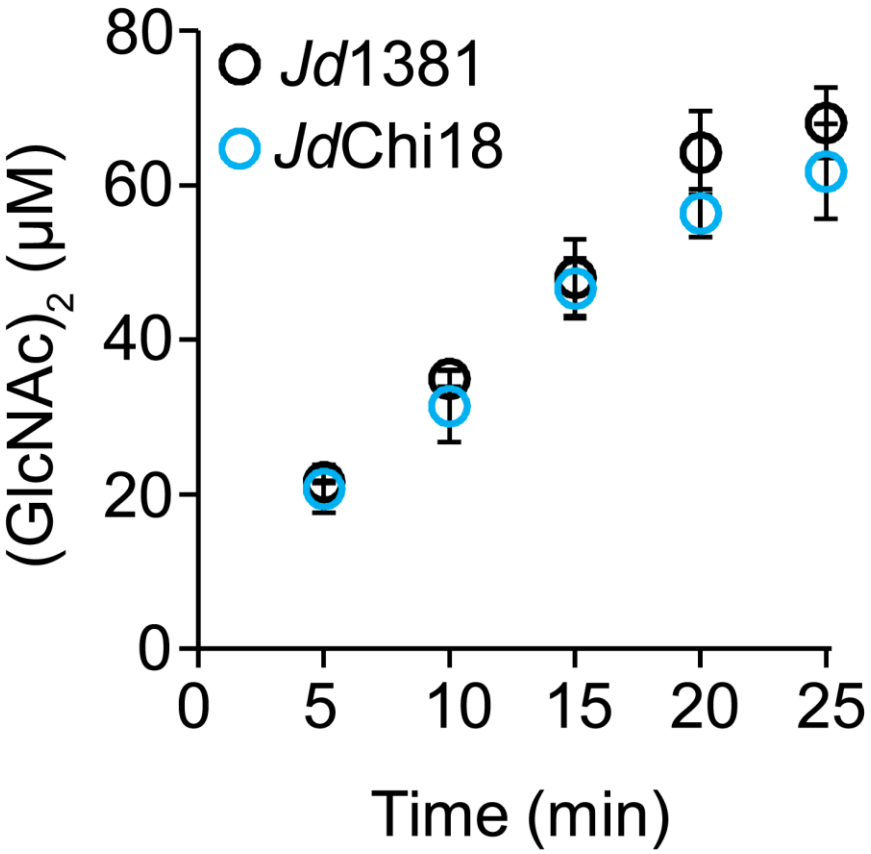

Figure S3. Kinetics of the degradation of chitopentaose by *Jd*1381 and *Jd*Chi18. The reaction mixture contained 100 μM chitopentaose and 5 nM enzyme in 20 mM BisTris pH 6.0 and reactions were incubated at 40 °C without shaking. Reactions carried out in the presence of 1 mM ascorbic acid gave the same result. Error bars indicate SD of experimental data (n = 3).

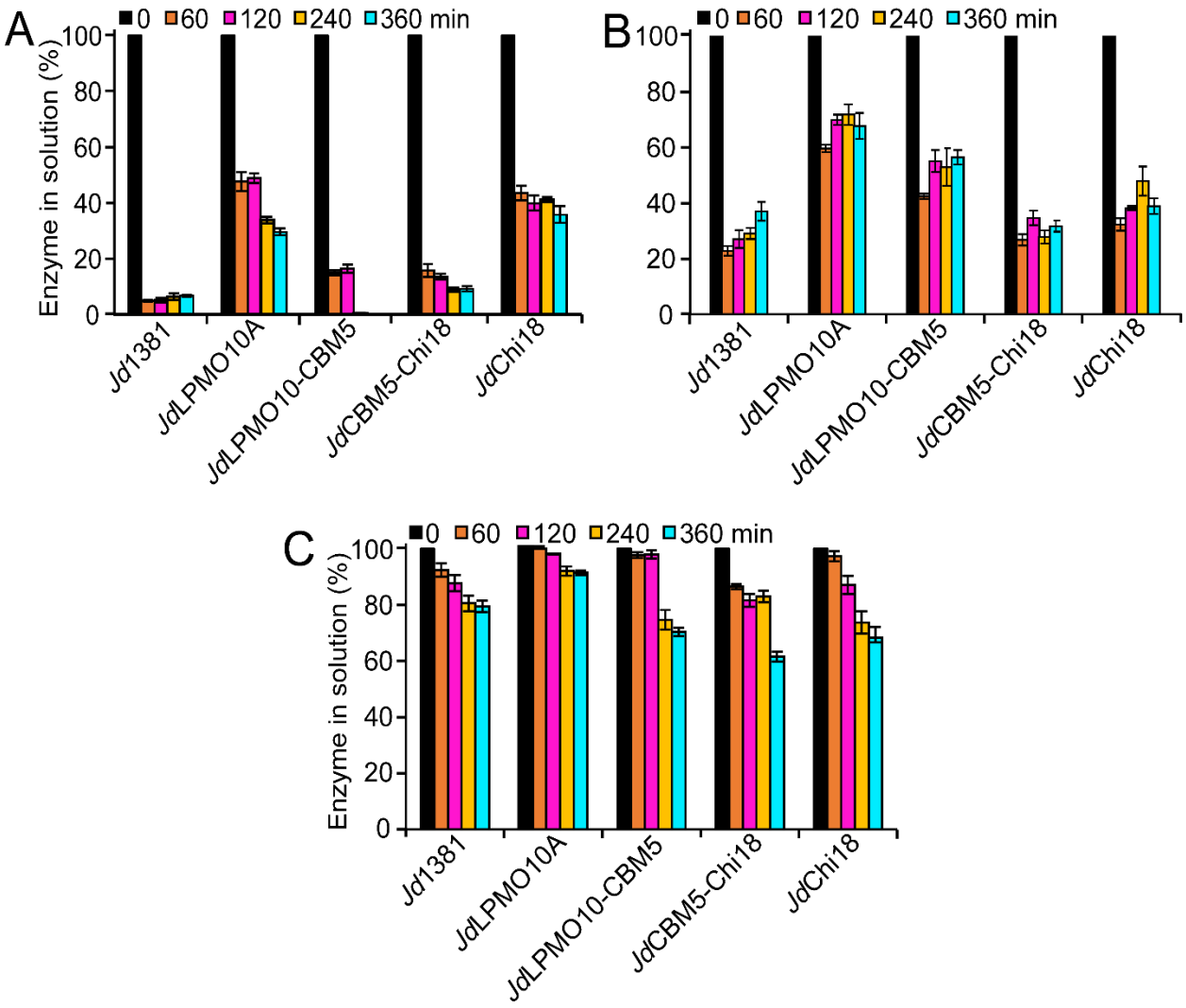

Figure S4. Time-dependent binding of *Jd*1381 variants to α-chitin (A) and β-chitin (B). Panel C shows control reactions without added chitin. For assessment of binding, reaction mixtures were sampled at specific time points and the concentrations of unbound enzymes in supernatants were determined using a Bradford Protein Assay Kit. The reaction mixtures contained 2 µM Cu(II)-saturated enzyme, 10 g/L α-chitin or β-chitin in 20 mM BisTris pH 6.0, and were incubated at 40 °C with shaking at 1000 rpm in the presence of 1mM AscA. All data points represent the mean of three independent experiments ± SD. Note that panel C indicates that some of the proteins are unstable in the absence of substrate. These stability effects were still very small at the first time point (60 min), while virtually maximum binding was observed at this timepoint in all cases (panels A and B). Therefore, possible stability effects were not taken into account when discussing the trends visible in panels A and B in the main text.

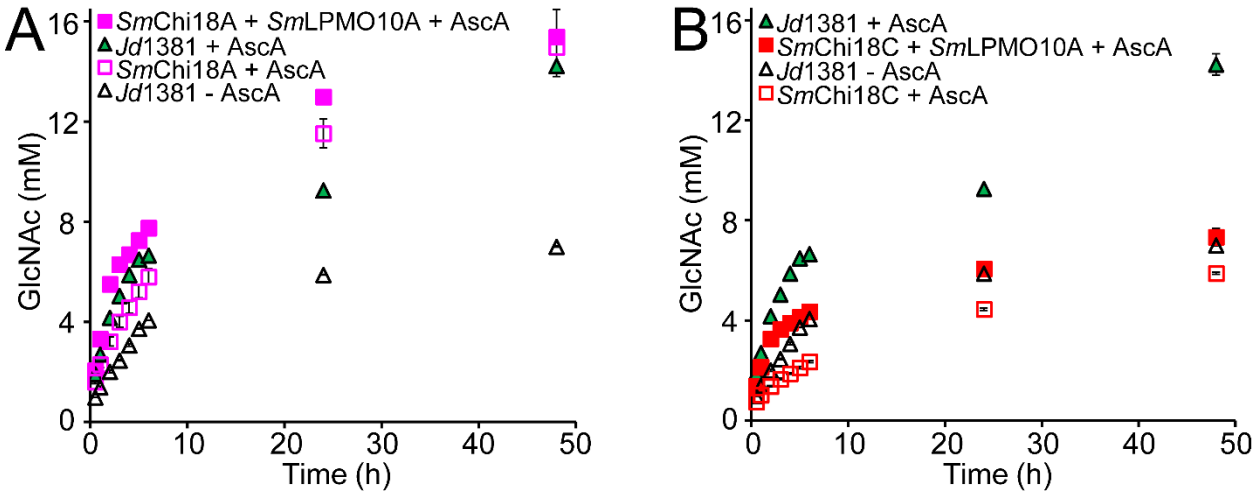

Figure S5. Comparison of *Jd*1381 with combinations of chitinases and an AA10-type LPMO from *Serratia marcescens* BJL200 in α-chitin hydrolysis. (A) Comparison of *Jd*1381 with a combination of *Sm*Chi18A (reducing end exo/processive chitinase) and *Sm*LPMO10A. (B) Comparison of *Jd*1381 with a combination of *Sm*Chi18C (endo/non-processive chitinase) and *Sm*LPMO10A. All reactions contained 1% α-chitin, 1µM of each enzyme, and 1 mM AscA (unless indicated otherwise), in 20 mM BisTris pH 6.0, and were incubated at 40 ºC. Before analysis, soluble products were converted to GlcNAc by overnight incubation with 1.5 µM *Sm*CHB (chitobiase, an *N*-acetylhexosaminidase) at 37 °C. Error bars indicate SD of experimental data (n = 3). Incubation of these chitin substrates under the same conditions but in the absence of enzyme did not yield detectable levels of soluble products.

3. SUPPORTING DISCUSSION.

Comparative assessment of the catalytic activity of *Jd*1381

Below, we describe the calculations used to roughly estimate the initial rate of *Jd*1381 and several previously described enzyme systems when acting on α-chitin. All cited studies used the same α-chitin, but did not usually correct for moisture and ash content when estimating enzyme dosages, yields and rates. In the discussion below, this correction, explained in the next paragraph, has been made.

The linear part of the green progress curve in Figure 4B shows that under the conditions used here, i.e. in the presence of AscA, *Jd*1381 converted the substrate at a rate of 6.7 % per hour. The substrate concentration after subtracting moisture (5.42 %) and ash (6.43 %) contents (10 g/L – 1.185 g/L = 8.815 g/L), expressed as chitobiose, was 21.7 mM; the enzyme concentration was 1 μM. If we assume, for the sake of simplicity, that all products generated by *Jd*1381 are chitobiose, a solubilization rate of 6.7 % per hour represents a chitobiose production rate of 0.067 x 21.7 = 1.45 mM per hour, leading to an apparent rate of $1.45 \times 10^{-3} / 1 \times 10^{-6} = 1.45 \times 10^{3}$ h^{-1} = 24 min^{-1} = 0.40 s^{-1}.

Expressed in other terms, in the experiment of Figure 4B, the protein loading was 66.3 mg per 8.815 g of chitin (the mass of *Jd*1381 is 66349 Da), or 7.52 mg/g, which, at this substrate concentration (8.815g/L) gave a turnover rate of 1.45 mM per hour.

Mekasha et al. (8) developed an optimized cocktail comprised of five *S. marcescens* enzymes (*Sm*ChiA, *Sm*ChiB, *Sm*ChiC, *Sm*LPMO10A and *Sm*CHB). At a total protein loading of 5.6 mg/g and a substrate concentration of 13.2 g/L (32.5 mM chitobiose), the initial rate of α-chitin degradation by this cocktail was in the order of 15 % per hour, or 4.87 mM per hour, so, about three times faster than *Jd*1381.

Forsberg et al. (9) studied degradation of α-chitin by *Sm*ChiC in the presence of *Cj*LPMO10A and ascorbic acid, using 0.5 μM of each of the enzymes (corresponding to 0.5 μM of *Jd*1381) and a substrate concentration of 8.815 g/L (21.7 mM chitobiose). Figure 8A in Forsberg et al., shows that the rate of chitobiose production was in the order of 0.5 mM per hour, which gives an apparent initial rate of 0.28 s^{-1}, which is lower than the rate calculated for *Jd*1381.

Mutahir et al. (10) studied degradation of α-chitin by a combination of *Sm*ChiA, *Sm*ChiB, *Sm*ChiC (0.25 μM of each) and a highly active four-domain LPMO10 (0.5 μM) from *Bacillus cereus* named *Bc*LPMO10A, using a substrate concentration of 8.815 g/L (21.7 mM chitobiose). Figure 5 in this study shows an approximate initial rate of 4 % conversion per hour, which equals 0.87 mM/hour, which, if we divide by 0.5 μM enzyme, leads to an apparent rate of 0.48 s^{-1}.

REFERENCES

1. Papanikolau, Y., Prag, G., Tavlas, G., Vorgias, C. E., Oppenheim, A. B., and Petratos, K. (2001) High resolution structural analyses of mutant chitinase A complexes with substrates provide new insight into the mechanism of catalysis. *Biochemistry* **40**, 11338-11343
2. Horn, S. J., Sørbotten, A., Synstad, B., Sikorski, P., Sørlie, M., Vårum, K. M., and Eijsink, V. G. H. (2006) Endo/exo mechanism and processivity of family 18 chitinases produced by *Serratia marcescens*. *FEBS J.* **273**, 491-503
3. Zakariassen, H., Aam, B. B., Horn, S. J., Vårum, K. M., Sørlie, M., and Eijsink, V. G. H. (2009) Aromatic residues in the catalytic center of chitinase A from *Serratia marcescens* affect processivity, enzyme activity, and biomass converting efficiency. *J. Biol. Chem.* **284**, 10610-10617
4. Igarashi, K., Uchihashi, T., Uchiyama, T., Sugimoto, H., Wada, M., Suzuki, K., Sakuda, S., Ando, T., Watanabe, T., and Samejima, M. (2014) Two-way traffic of glycoside hydrolase family 18 processive chitinases on crystalline chitin. *Nat. Commun.* **5**, 3975
5. Jana, S., Hamre, A. G., Wildberger, P., Holen, M. M., Eijsink, V. G. H., Beckham, G. T., Sørlie, M., and Payne, C. M. (2016) Aromatic-mediated carbohydrate recognition in processive *Serratia marcescens* chitinases. *J. Phys. Chem. B.* **120**, 1236-1249
6. Payne, C. M., Baban, J., Horn, S. J., Backe, P. H., Arvai, A. S., Dalhus, B., Bjørås, M., Eijsink, V. G. H., Sørlie, M., Beckham, G. T., and Vaaje-Kolstad, G. (2012) Hallmarks of processivity in glycoside hydrolases from crystallographic and computational studies of the *Serratia marcescens* chitinases. *J. Biol. Chem.* **287**, 36322-36330
7. DeLano, W., and Lam, J. W. (2005) A communications tool for computational models. *Abstr. Pap. Am. Chem. S.* **230**, U1371-U1372
8. Mekasha, S., Byman, I. R., Lynch, C., Toupalová, H., Anděra, L., Næs, T., Vaaje-Kolstad, G., and Eijsink, V. G. H. (2017) Development of enzyme cocktails for complete saccharification of chitin using mono-component enzymes from *Serratia marcescens*. *Process Biochem.* **56**, 132-138
9. Forsberg, Z., Nelson, C. E., Dalhus, B., Mekasha, S., Loose, J. S., Crouch, L. I., Røhr, A. K., Gardner, J. G., Eijsink, V. G. H., and Vaaje-Kolstad, G. (2016) Structural and functional analysis of a lytic polysaccharide monooxygenase important for efficient utilization of chitin in *Cellvibrio japonicus. J. Biol. Chem.* **291**, 7300-7312
10. Mutahir, Z., Mekasha, S., Loose, J. S. M., Abbas, F., Vaaje-Kolstad, G., Eijsink, V. G. H., and Forsberg, Z. (2018) Characterization and synergistic action of a tetra-modular lytic polysaccharide monooxygenase from *Bacillus cereus*. *FEBS Lett* **592**, 2562-2571